RPE Radiation Physics & Engineering
An International Peer-Reviewed Journal
Published by K.N. Toosi University of Technology
http://rpe.kntu.ac.ir
Research Article

Radiation Physics and Engineering 2021; 2(1):27–33
https://doi.org/10.22034/rpe.2021.202211.1025

Dosimetric investigation of esophageal stents carrying I-125 seeds for the treatment of advanced esophageal cancer

Payman Rafiepour[a,*], Shahab Sheibani[b], Daryiush Rezaey Uchbelagh[c], Hossein Poorbaygi[a]

[a] *Department of Nuclear Engineering, School of Mechanical Engineering, Shiraz University, Shiraz, Iran*
[b] *Nuclear Science Research School, Nuclear Science and Technology Research Institute (NSTRI), Tehran, Iran*
[c] *Department of Energy Engineering and Physics, Amirkabir University of Technology, Tehran, Iran*

HIGHLIGHTS

- 2-D and 3-D dose distributions of I-125 seed-loaded esophageal stents were obtained.
- The dose to the OARs was calculated by simulating a MIRD male phantom.
- Seed-loaded stents with 15-20 mm inter-seed spacing, show appropriate dose distributions.

ABSTRACT

Radioactive stents loaded with I-125 seeds have been widely used for the treatment of advanced esophageal cancer. Understanding the dose distribution of such stents before the clinical use is essential. This study provides a dosimetric investigation of I-125 seed-loaded stents based on the seed's arrangement and activity. A cylindrical water equivalent phantom with an esophageal stent loaded with I-125 seeds, were employed. The seeds arrangements were determined based on the distance between the centers of two adjacent seeds (z) along the stent length. EBT3 films as well as Geant4 Monte Carlo toolkit were used to obtain the dose distribution around the stent. By modeling the MIRD phantom, the dose delivered to the related organs at risk was calculated. The appropriate dose distribution is achieved for $z = 15$ mm, in which the absorbed dose at a depth of 5 mm reaches about 45% of the absorbed dose near the stent surface, thereby the therapeutic dose is delivered to the reference points. Both arrangements ($z = 15$ and 20 mm) seemed to be clinically eligible and their utilization depends on the patient and the hospital facilities. Using esophageal stents with $z > 20$ mm is not recommended due to the presence of cold spots in the dose distribution.

KEYWORDS
Esophageal cancer
Radioactive stent
Brachytherapy
Dosimetry
Monte Carlo

HISTORY
Received: 10 October 2020
Revised: 14 December 2020
Accepted: 17 December 2020
Published: January 2021

1 Introduction

Esophageal cancer is one of the most common cancers in the world. Challenging the advanced esophageal cancer, in which cancerous tumors invade nearby tissues and finally causes death, is one of the current concerns of the physicians. Over 455000 new esophageal cancer cases and 400000 deaths were reported in 2012 worldwide (Torre et al., 2015). The most common symptom of advanced esophageal cancer is dysphagia and the use of self-expandable metal stents is the safest solution. Recently the combination of esophageal stents and brachytherapy has been studied for the treatment of advanced esophageal cancer. The placement of I-125 brachytherapy seeds on the esophageal stent, helps to palliate dysphagia as well as to prevent the inner growth of tumor in the stent (Guo et al., 2007, 2008). As recommended by the American Association of Physicists in Medicine (AAPM) TG60 and TG149 reports, understanding the dose distribution of any radioactive stent is necessary before the clinical use (Nath et al., 1999; Chiu-Tsao et al., 2007). Won *et al.* developed a radioactive esophageal stent impregnated with Ho-166 and computed the dose distribution by the Electron Gamma Shower (EGS4) code. They also performed experimental studies with beagle dogs (Won et al., 2002, 2005). Chu *et al.* investigated the radiation field surrounding the Re-188 esophageal stent, using thermo-luminescent dosimeters (TLDs) (Chu et al., 2008).

There are several clinical studies that indicate the potential benefits of I-125 seed-loaded esophageal stents in the palliation of dysphagia and improvement of the survival time of patients (Zhu et al., 2014; Zhongmin et al.,

*Corresponding author: pa.rafiepour@gmail.com

2012; Liu et al., 2014). Yao *et al.* used TLDs, Monte Carlo N-Particle eXtended (MCNPX) code and treatment planning software to evaluate the dose distribution of biliary stents loaded with I-125 seeds (Yao et al., 2017). However, few publications carried out dosimetric investigation for I-125 seed-loaded stents. Therefore, more studies on the dose distribution of radioactive esophageal stents carrying I-125 seeds is needed, based on the arrangement and the activity of the seeds as well as the dose delivery to organs at risk (OARs). This work performs a dosimetric investigation of such stents, using radiochromic EBT3 films and Geant4 simulation toolkit. The results of the simulation were compared with experimental measurements.

2 Materials and Methods

2.1 Radioactive seeds

I-125 IR-Seed Model brachytherapy seeds manufactured in the Nuclear Science and Technology Research Institute of Atomic Energy Organization, were employed in this study. This model has a silver cylindrical core with 0.5 mm in diameter and 3 mm in length. I-125 is uniformly coated on the surface of the core surrounded with 0.05 mm titanium shield. The full length and diameter of the source is 4.6 and 0.8 mm, respectively (Lohrabian et al., 2013). The seed's initial activity was 0.44 ± 0.06 mCi. The nuclear data for I-125 for dosimetry, recommended by AAPM are presented in Table 1 (Rivard et al., 2004).

Table 1: Recommended nuclear data for I-125 source (half-life=59.4 days) for dosimetry.

Photon energy (keV)	Abundance (%)
40.6	27.202
75.7	27.472
20.2	30.98
4.39	31.71
6.68	35.492

2.2 Esophageal stents

Nitinol (55.8% Ni, 44.2% Ti) esophageal stent, model ESO-1-24-100 (Endo-flex), was used in this study (Fig. 1). It has 120 mm length and 24 mm diameter. A plastic sheath was utilized to fix the positions of the seeds on the stent. The seed positions were determined by cutting eight grooves with 40 mm length and 1 mm width on the plastic sheath (with angular distances of 45 degrees).

The seeds were inserted with specific arrangements (Fig. 2). The spaces between the seeds were filled with silicon spacers. Every four seeds, as a group, were arranged in a plane perpendicular to the stent axis with an angular distance of 90 degrees. Each group was rotated 45 degrees relative to the adjacent groups. The center to center distance of the two adjacent seeds, z, was fixed.

Figure 1: (a) Loading the esophageal stent with I-125 seeds, and (b) The dimensions of the stent.

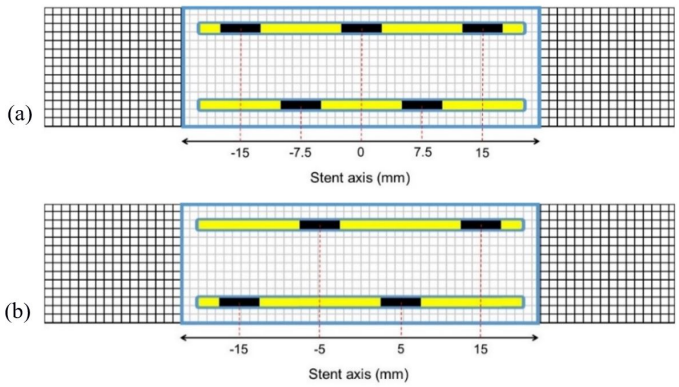

Figure 2: The arrangements of I-125 seeds in the plastic tubes with (a) z=15 mm, (b) z=20 mm.

2.3 Radiocromic EBT3 film calibration and scan

Radiochromic EBT3 film is a new member of EBT series radiochromic films, developed to be more accurate and reliable. It has a symmetrical structure composed of three layers: an active layer with 28 μm thickness between two Matte Polyester layers with 125 μm thickness. They have benefits of high spatial resolution (in the order of submillimeter), small energy dependence and near tissue equivalence, which make them desirable for radiation fields with steep dose gradients. The Newton rings effect due to the direct contact of the film with the glass surface of the scanner was eliminated in EBT3 film by embedding silica particles within its polyester layers (Devic et al., 2016). In this study the sheets of EBT3 film were cut into 5×2.5 cm^2 pieces and inserted in phantom in contact with an I-125 seed-loaded esophageal stent.

For calibration, ten pieces of 2×2 cm^2 were cut from the same sheet and exposed by an X-ray tube machine (50 kV), in air at a distance of 100 cm from the source. A range of doses from 0.5 to 10 Gy was delivered to the films. The films were marked to keep the same orientation for all pieces. One piece of film was kept unexposed for background measurement. All the films were stored in a safe place for 24 hours before processing to ensure the response stability (Devic et al., 2016).

Microtek ScanMaker 9800XL plus (Microtek International Inc., Hsinchu, Taiwan) flatbed scanner, was used in this work. Two artifacts have been reported by using

flatbed scanners as a radiochromic film readout system: The orientation effect (the dependence of scanner response on the orientation of the film on the scanner bed) and the lateral effect (the parabolic change of scanner response by the lateral distance from the scanner midline) (Schoenfeld et al., 2014). Prior to scanning, the scanner was warmed up by several empty scans before digitizing the calibration films. All EBT3 film pieces were located at the center of the scanning bed and in a same orientation to reduce these artifacts (Devic et al., 2016). Also the Callier effect due to the flatness of the film on the scan window may affect the film response (Chavel and Lowenthal, 1978), but new scanners have a pressed glass sheet on the inner surface of their lid to mitigate this effect. The irradiated films were digitized using RGB 48-bit mode (16-bit color depth per Red, Green and Blue color channel) with 100 dots per inch (dpi) scanning resolution in transmission mode. Images were saved in uncompressed tagged image file format (TIFF). The mean pixel value (PV) of a region of interest (ROI) of 1.5×1.5 cm^2 was read with ImageJ software. All PVs were obtained in red channel due to the highest sensitivity of active layer to the red wave length (Devic et al., 2016). The net optical density (nOD) was calculated by Eq. (1):

$$\mathrm{nOD} = \log_{10}(\mathrm{PV}_{bef}/\mathrm{PV}_{aft}) \tag{1}$$

in which, PV_{bef} and PV_{bef} are the average PVs over the ROI of scanned images before and after exposure, respectively. Substituting the nOD of each point of the measurement film image into the calibration equation (Eq. (2)), gives the absorbed dose in that point. Then, dose rate is calculated by Eq. (2):

$$\dot{D}(\mathrm{Gy/h}) = \frac{D}{T_{irr}} \times \mathrm{e}^{-\lambda T_{irr}} \tag{2}$$

where D (in Gy) is the dose obtained by calibration curve equation, T_{irr} (in h) is the exposure time and λ (in h^{-1}) is the decay constant equal to $0.693/T_{1/2}$. The exponential term is a correction factor implemented due to the decay of I-125 during the exposure time. T_{irr} for arrangements 1 (z=15 mm) and 2 (z=20 mm) was 91 hours and 146 hours, respectively.

2.4 Water equivalent phantom

The cylindrical water equivalent ($Z_{eff,\mathrm{PMMA}}$=6.48) phantom with a density of 1.18 g.cm^{-3} was employed in this work. There is a hollow cylinder in the phantom with diameter of 2.4 cm to easily accommodate the esophageal stent (Fig. 3). The films were cut and inserted in the phantom very carefully to minimize the positioning uncertainties.

2.5 Monte Carlo simulation

Geant4.10.2 simulation toolkit with electromagnetic low energy physics "emstandard_opt3", was implemented in this study. The emstandard_opt3 package uses the most accurate standard and low-energy models. The low energy package includes photoelectric effect, Compton scattering, Rayleigh scattering, bremsstrahlung, ionization and fluorescence emission (Agostinelli et al., 2003).

Esophageal stent loaded with I-125 seeds is composed of a bare Nitinol stent with density of 6.45 g.cm^{-3}, a polymeric covering membrane and Nitinol sheaths (4.61×0.81×0.81 mm^3) containing seeds. The radioactive stent was simulated in the center of a cylindrical water phantom similar to the setup shown in Fig. 3. Using Geant4 cylindrical mesh, the phantom was divided into 0.5 mm thickness concentric rings along the stent axis. Each division was performed for different radial distances. Furthermore, spherical detectors with 0.5 mm diameter were defined at 2, 3, 5, 7, 10, 15 and 20 mm from the stent surface to compare with EBT3 dose rate measurements. The simulated stent (z=15 mm) is shown in Fig. 4-a. With 5×10^8 primary particles, all statistical uncertainties in Geant4 simulations were below 4%, up to depth of 10 mm. The total activity of the stent was considered to be equal to the sum of seeds activities. Another simulation was performed by modeling the MIRD male phantom (Snyder et al., 1969), to calculate the dose delivered to OARs (Fig. 4-b). The total doses delivered to OARs are tabulated in Table 2.

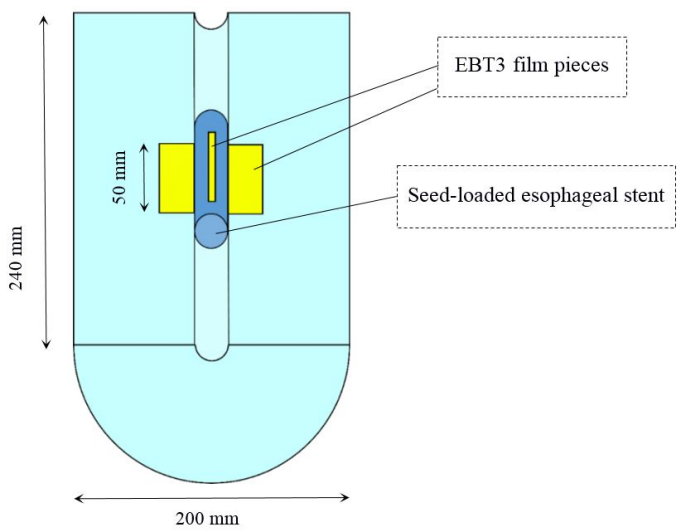

Figure 3: PMMA phantom with radioactive stent (blue cylinder) and EBT3 films.

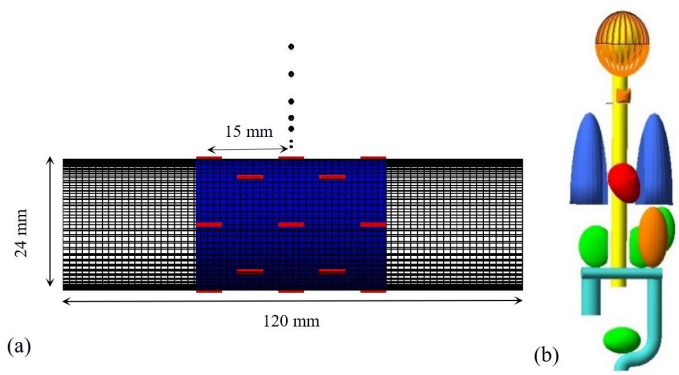

Figure 4: The simulated (a) esophageal stent loaded with I-125 seeds with spherical detectors and (b) the MIRD male phantom.

Table 2: The total dose delivered (Gy) to the OARs from esophageal stents carrying I-125 seeds, obtained by Geant4.

OAR	z=10 mm (28 seeds)			z=15 mm (20 seeds)			z=20 mm (16 seeds)		
	0.4 mCi	0.5 mCi	0.6 mCi	0.4 mCi	0.5 mCi	0.6 mCi	0.4 mCi	0.5 mCi	0.6 mCi
Thyroid	12.163	15.204	18.244	8.688	10.860	13.032	6.950	8.688	10.425
Lung	1.730	2.163	2.595	1.236	1.545	1.854	0.988	1.236	1.483
Heart	0.625	0.781	0.938	0.446	0.558	0.670	0.357	0.446	0.536
Spinal cord	0.169	0.211	0.253	0.120	0.150	0.181	0.096	0.120	0.144
Kidney	0.0046	0.0057	0.007	0.0032	0.0041	0.0049	0.0026	0.0032	0.004

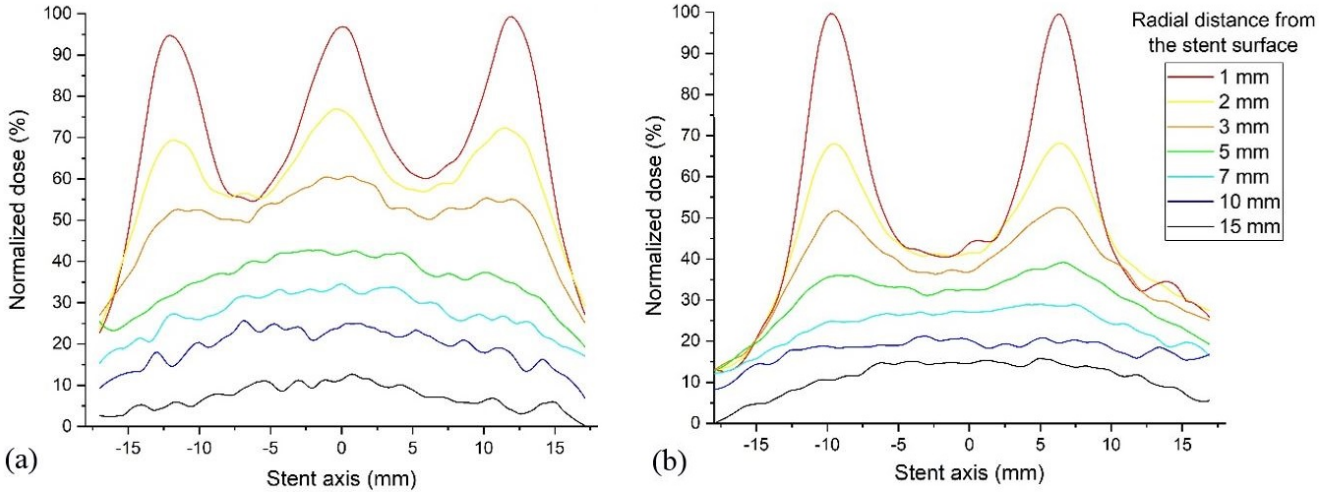

Figure 5: Dose profiles of the esophageal stents carrying I-125 seeds for different depths (1, 2, 3, 5, 7, 10 and 15 mm), obtained by EBT3 films. (a) z=15 mm (20 seeds), z=20 mm (16 seeds).

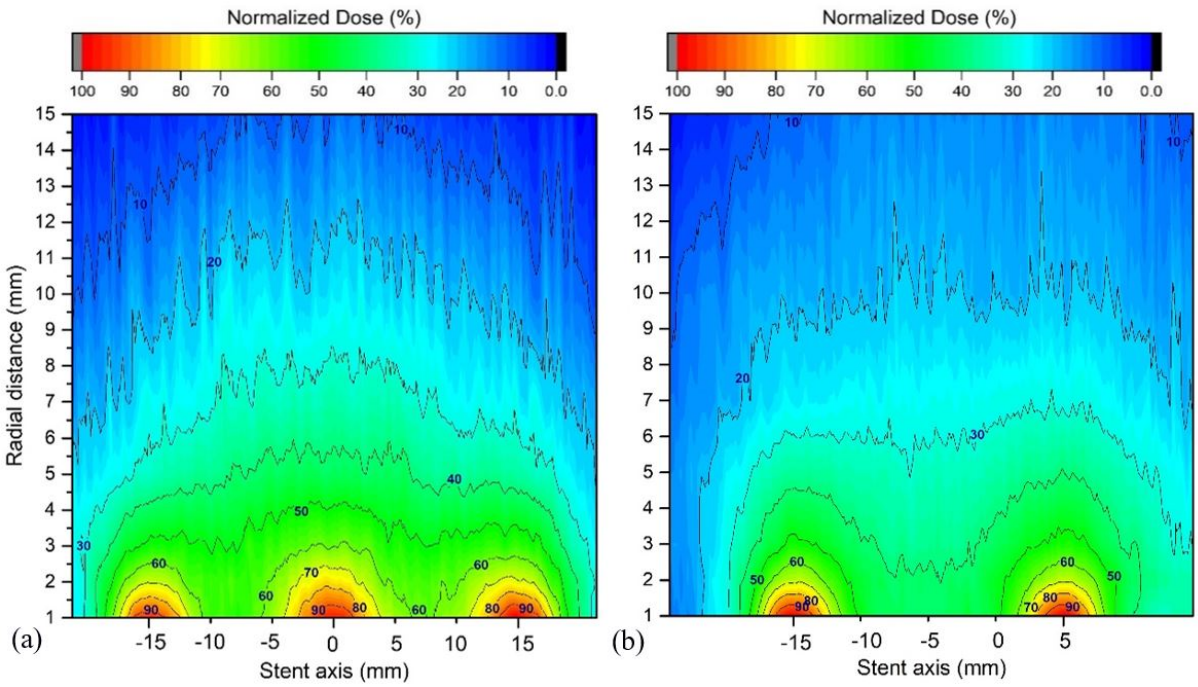

Figure 6: 3D dose distribution of the esophageal stents loaded with I-125 seeds obtained by EBT3 films. (a) z=15 mm (20 seeds), (b) z=20 mm (16 seeds).

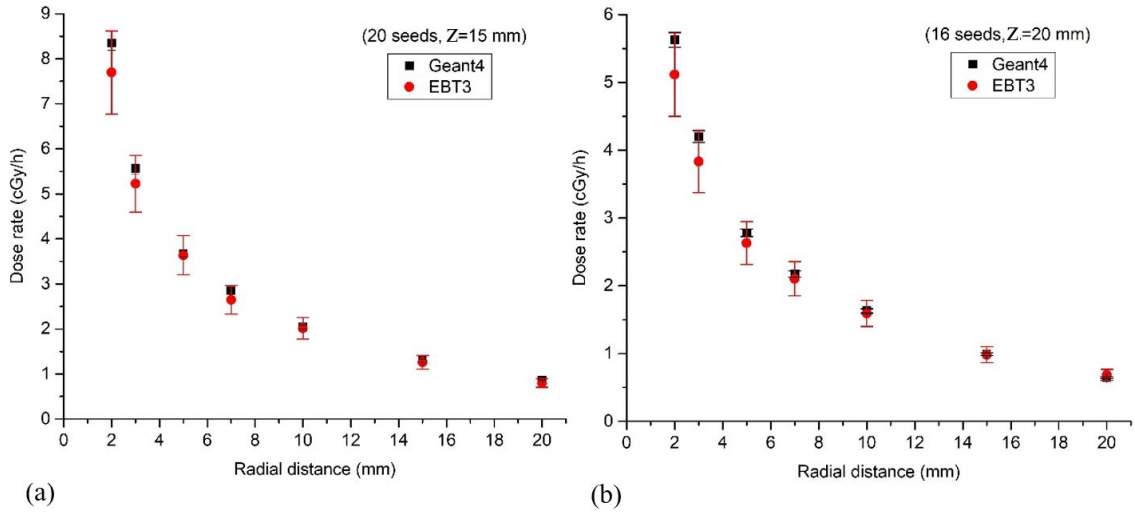

Figure 7: A comparison between dose rates obtained experimentally and by Monte Carlo simulation. (a) z=15 mm (20 seeds), (b) z=20 mm (16 seeds).

3 Results

EBT3 film calibration curve was obtained by plotting dose vs nOD. Data were fitted with a polynomial function to achieve Eq. (3):

$$D = 554.59(\text{nOD})^3 - 36.045(\text{nOD})^2 + 15.12(\text{nOD}) + 0.064 \ , \ (R^2 = 0.999) \quad (3)$$

The dose distributions of esophageal stents loaded with I-125 seeds are represented in Figs. 5 and 6. The uncertainties that are involved include uncertainty originated from handling films, the measured response of the film to radiation and the fitting procedure of the calibration curve. Other sources of error consist of phantom and stent wrong assembly, X-ray tube error in exposure and lack of uniform exposure to the reference films. We tried to keep the total uncertainty below 5%. Figure 7 shows a comparison of dose rates measured experimentally and by simulation.

As radioactive esophageal stents are permanent implant in the case of advanced esophageal cancer, their total accumulated dose is of importance. The accumulated dose of I-125 seed-loaded stents with different seed arrangements and activities (mCi) are presented in Table 3. Dose reference point in clinical applications is usually considered at 5 mm from the stent surface and the prescription dose is reported to be 40 to 50 Gy (Zhu et al., 2014; Gaspar et al., 1997; Zhu et al., 2012). However, the prescribed dose up to 80 Gy has also been reported (Lu et al., 2017; Huimin et al., 2015).

The dose per decay delivered to heart, kidney, lung, stomach, thyroid, and spinal cord was 2.3×10^{-5} nGy, 2.03×10^{-8} nGy, 2.51×10^{-11} nGy, 5.63×10^{-8} nGy, 1.49×10^{-10} nGy, 3.96×10^{-7} nGy, and 5.5×10^{-9} nGy, respectively. Table 2 shows the accumulated doses, received by OARs from esophageal seed-loaded stents with different seed activities.

4 Discussion

As it is shown in the dose distributions in Figs. 5 and 6, the high gradient of dose decreases as the radial distance from the stent surface increases. The absorbed dose at the reference point is approximately 40% of that of at the depth of 1 mm. In the case of second arrangement (z=20 mm), dose distribution at 5 mm from the stent surface shows greater changes than that of the arrangement 1. The difference of absorbed dose at the location of a seed and the adjacent vacant place reaches to 13 to 22%. While for the arrangement 1, this difference is not obvious and the distribution of dose at the reference point has almost reached a perfect uniformity. The lack of uniformity especially at the reference depth is not clinically desirable, due to the appearance of cold spots between the seeds which increases the probability of the tumor recurrence. Such arrangements shown in Fig. 2 helps to overcome this non-uniformity. Figure 6 illustrates that for z=15 mm, there is an intensity equal to 50% of the dose near the stent surface, uniformly extends along the length of the stent. But for z=20 mm, even an intensity equal to 40% of the dose near the surface shows a significant variation.

A good agreement was achieved between EBT3 films and Geant4 results. The relative errors of obtained dose rates were below 10% for all radial distances (Fig. 7). Dose rates at the reference point calculated by EBT3 film measurements were 3.64 cGy.h^{-1} and 2.63 cGy.h^{-1} for z=15 mm and 20 mm, respectively. The corresponding Geant4 results were 3.66 cGy.h^{-1} and 2.78 cGy.h^{-1}, respectively. According to Fig. 7 and the accumulated doses shown in Table 3, the total absorbed dose at the reference depth is more than 40% of the dose at the stent surface, indicated the good potential of I-125 sources to penetrate the esophagus wall and deliver a therapeutic dose to the tumor. However, the high range photons of I-125 may lead to radiation damage to healthy tissues near the tumor. Dose uniformity can be obtained by reducing z, but there is a limitation on changing z. To cover the entire

Table 3: Accumulated dose (Gy) of esophageal stents carrying I-125 seeds at different radial distances from the stent surface for different seed activities, obtained by Geant4.

Depth	z=10 mm (28 seeds)			z=15 mm (20 seeds)			z=20 mm (16 seeds)		
(cm)	0.4 mCi	0.5 mCi	0.6 mCi	0.4 mCi	0.5 mCi	0.6 mCi	0.4 mCi	0.5 mCi	0.6 mCi
1	204.6	255.7	306.9	146.4	183.0	219.7	115.8	144.7	173.7
5	97.1	121.3	145.6	69.5	86.9	104.3	54.9	68.6	82.4
10	53.3	66.6	79.9	38.1	47.6	57.1	30.0	37.5	45.0
15	32.9	41.1	49.3	23.4	29.3	35.1	18.4	23.0	27.7
20	22.4	28.0	33.6	15.9	19.9	23.9	12.5	15.7	18.8

lesion of the tumor with the I-125 seeds, at least 2 cm exceeding the tumor margins is required (Guo et al., 2008; Zhongmin et al., 2012). By decreasing z, therefore increasing the number of seeds, their activities should be reduced compared to the previous state. Otherwise, a large dose will be delivered to the esophagus wall. The number, the arrangement and the activity of brachytherapy seeds should be determined by treatment planning system based on the size and the location of tumor. Table 3 shows that decreasing z leads to an increase in the number of seeds on the stent, therefore increases the absorbed dose at the reference points and the damage to healthy tissues near the tumor. It can be inferred from table 3 that more seed activities may be used clinically, because the delivered doses to OARs are below their dose constraints (Brady and Perez, 2013).

5 Conclusion

Present work performs a dosimetric investigation of esophageal stents loaded with I-125 IR-Seed model seeds, using radiochromic EBT3 films and Geant4 toolkit. The results indicate that the appropriate dose distribution is achieved for z=15 mm, in which the absorbed dose at a depth of 5 mm reaches about 45% of the dose intensity near the stent surface, thereby a therapeutic dose (50 to 140 Gy) depends on the seeds activity, is delivered to the reference points. Note that both arrangements shown in Fig. 2 seem to be clinically eligible and their utilization depends on the patient (the stage of esophageal cancer) and the hospital facilities. Due to the presence of cold spots at the spaces between the seed, utilizing of I-125 seed-loaded stents with more than 20 mm is not recommended. The calculations and results related to the dose distribution of esophageal stents loaded with I-125 IR-Seed model seeds, can be implemented in treatment planning system.

References

Agostinelli, S., Allison, J., Amako, K. a., et al. (2003). GEANT4a simulation toolkit. *Nuclear Instruments and Methods in Physics Research Section A: Accelerators, Spectrometers, Detectors and Associated Equipment*, 506(3):250–303.

Brady, L. W. and Perez, C. A. (2013). *Perez & Brady's principles and practice of radiation oncology*. Lippincott Williams & Wilkins.

Chavel, P. and Lowenthal, S. (1978). Noise and coherence in optical image processing. I. The Callier effect and its influence on image contrast. *JOSA*, 68(5):559–568.

Chiu-Tsao, S.-T., Schaart, D. R., Soares, C. G., et al. (2007). Dose calculation formalisms and consensus dosimetry parameters for intravascular brachytherapy dosimetry: Recommendations of the AAPM Therapy Physics Committee Task Group No. 149. *Medical Physics*, 34(11):4126–4157.

Chu, J., Jin, J., Ni, S., et al. (2008). Radiation field feature of ^{188}Re esophageal stent. *Nuclear Medicine Communications*, 29(5):462–464.

Devic, S., Tomic, N., and Lewis, D. (2016). Reference radiochromic film dosimetry: review of technical aspects. *Physica Medica*, 32(4):541–556.

Gaspar, L. E., Nag, S., Herskovic, A., et al. (1997). American Brachytherapy Society (ABS) consensus guidelines for brachytherapy of esophageal cancer. Clinical Research Committee, American Brachytherapy Society, Philadelphia, PA. *International Journal of Radiation Oncology, Biology, Physics*, 38(1):127–132.

Guo, J.-H., Teng, G.-J., Zhu, G.-Y., et al. (2007). Self-expandable stent loaded with ^{125}I seeds: feasibility and safety in a rabbit model. *European Journal of Radiology*, 61(2):356–361.

Guo, J.-H., Teng, G.-J., Zhu, G.-Y., et al. (2008). Self-expandable esophageal stent loaded with ^{125}I seeds: initial experience in patients with advanced esophageal cancer. *Radiology*, 247(2):574–581.

Huimin, Y., Zhang, H., Ding, B., et al. (2015). Esophageal stent covered with radioactive ^{125}I seeds arranged at different distance: dosimetric; comparison study. *Journal of Interventional Radiology*, (4):338–341.

Liu, N., Liu, S., Xiang, C., et al. (2014). Radioactive self-expanding stents give superior palliation in patients with unresectable cancer of the esophagus but should be used with caution if they have had prior radiotherapy. *The Annals of thoracic surgery*, 98(2):521–526.

Lohrabian, V., Sheibani, S., Aghamiri, M. R., et al. (2013). Determination of dosimetric characteristics of irseed ^{125}I brachytherapy source. *Iranian Journal of Medical Physics*, 10(2):109–117.

Lu, J., Guo, J.-H., and Teng, G.-J. (2017). A novel irradiation stent for the treatment of malignant hilar biliary obstruction: A case series. *Brachytherapy*, 16(3):S49.

Nath, R., Amols, H., Coffey, C., et al. (1999). Intravascular brachytherapy physics: report of the AAPM Radiation Therapy Committee Task Group No. 60. *Medical Physics*, 26(2):119–152.

Rivard, M. J., Coursey, B. M., DeWerd, L. A., et al. (2004). Update of AAPM Task Group No. 43 Report: A revised AAPM protocol for brachytherapy dose calculations. *Medical Physics*, 31(3):633–674.

Schoenfeld, A. A., Poppinga, D., Harder, D., et al. (2014). The artefacts of radiochromic film dosimetry with flatbed scanners and their causation by light scattering from radiation-induced polymers. *Physics in Medicine & Biology*, 59(13):3575.

Snyder, W. S., Ford, M. R., Warner, G. G., et al. (1969). Estimates of absorbed fractions for monoenergetic photon sources uniformly distributed in various organs of a heterogeneous phantom. Technical report, Oak Ridge National Lab., Tenn.

Torre, L. A., Bray, F., Siegel, R. L., et al. (2015). Global cancer statistics, 2012. *CA: a cancer journal for clinicians*, 65(2):87–108.

Won, J. H., Lee, J. D., Wang, H. J., et al. (2002). Self-expandable covered metallic esophageal stent impregnated with beta-emitting radionuclide: an experimental study in canine esophagus. *International Journal of Radiation Oncology* Biology* Physics*, 53(4):1005–1013.

Won, J. H., Lee, J. D., Wang, H. J., et al. (2005). Effects of a holmium-166 incorporated covered stent placement in normal canine common bile ducts. *Journal of Vascular and Interventional Radiology*, 16(5):705–711.

Yao, L.-H., Wang, J.-J., Shang, C., et al. (2017). In vitro dosimetric study of biliary stent loaded with radioactive ^{125}I seeds. *Chinese Medical Journal*, 130(9):1093.

Zhongmin, W., Xunbo, H., Jun, C., et al. (2012). Intraluminal radioactive stent compared with covered stent alone for the treatment of malignant esophageal stricture. *Cardiovascular and Interventional Radiology*, 35(2):351–358.

Zhu, H.-D., Guo, J.-H., Mao, A.-W., et al. (2014). Conventional stents versus stents loaded with iodine-125 seeds for the treatment of unresectable oesophageal cancer: a multicentre, randomised phase 3 trial. *The Lancet Oncology*, 15(6):612–619.

Zhu, H.-D., Guo, J.-H., Zhu, G.-Y., et al. (2012). A novel biliary stent loaded with ^{125}I seeds in patients with malignant biliary obstruction: preliminary results versus a conventional biliary stent. *Journal of Hepatology*, 56(5):1104–1111.